Modification of the surface electronic structure of Cu(111) by monolayer Ni adsorption and the effects on H_2 chemisorption

K. H. Frank, R. Dudde, and H. J. Sagner
Fritz-Haber-Institut der Max-Planck-Gesellschaft, Faradayweg 4-6, D-1000 Berlin 33, Federal Republic of Germany

W. Eberhardt*
Berliner Elektronenspeicherring-Gesellschaft für Synchrotronstrahlung m.b.H., Lentzeallee 100, D-1000 Berlin 33, Federal Republic of Germany

(Received 15 August 1988)

We have used angle-resolved photoemission and k-resolved inverse photoemission to determine the electronic structure of a monolayer of Ni atoms grown epitaxially on Cu(111). At the center of the surface Brillouin zone (SBZ), the Ni-derived two-dimensional electronic structure exhibits three occupied bands and one empty band. This finding is consistent with a tight-binding calculation by Tersoff and Falicov, with the exception that the film is not magnetically "dead." The Λ_1 intrinsic surface-state band of Cu(111) is found to persist in the presence of the Ni overlayer without changing its binding energy or dispersion. The high density of Ni d-derived holes at E_F is responsible for the ability of the 1-ML Ni(1×1)/Cu(111) surface to dissociate molecular hydrogen, which is prevented by a dissociation barrier on the bare Cu(111) surface (ML denotes monolayer). In addition, we show that molecular hydrogen does not dissociate upon contact with an epitaxially grown monolayer of Cu atoms on Ni(111). In this case the Ni d holes are still existent but do not interact with the oncoming H_2 molecules because they are covered by the Cu overlayer. This proves the highly localized character of the hydrogen-dissociation process on transition-metal surfaces.

I. INTRODUCTION

Bimetallic transition-metal–overlayer systems present a scientific challenge in basic research as well as technology with respect to understanding both their catalytic and magnetic properties. The formation of the two-dimensional electronic structure of epitaxial monolayers, the development of bulk properties with increasing film thickness, the creation of electronic interface states, and the interaction with the underlying substrates are different aspects in studies of these epitaxial films. Among the large manifold of these systems the electronic, magnetic, and chemisorption properties of thin Ni overlayers on Cu surfaces have been of increasing interest in the past few years. The experimental work in this area[1,2] has been stimulated by extensive theoretical studies of the electronic structure or ordered overlayers.[3,4] With respect to chemisorption, the question has also been addressed how the surface magnetism is influenced by chemisorption[5] and how, on the other hand, the surface modification in the overlayer system might influence the chemisorption properties.[6]

The interaction of H_2 with transition-metal surfaces has been viewed as a prototypical system for the understanding of chemisorption. Moreover, this system is not only relevant for catalysis but also in materials science with respect to hydrogen storage or embrittlement. Two basic steps are involved in the hydrogen chemisorption process. First, the hydrogen molecule has to be dissociated and then atomic hydrogen is bound to the surface or may penetrate into the bulk of the metal depending on the heat of solution. Several theoretical and experimental studies have dealt with these phenomena on bare transition-metal surfaces previously.[7] On Ni surfaces H_2 spontaneously dissociates,[8] whereas on Cu surfaces H atoms are bound only after dissociating the molecule prior to adsorption.[9] The desorption temperature and the binding energy of H atoms on both these surfaces are actually quite similar.[8,9] The difference is in the existence of a *dissociation barrier* on Cu surfaces. The height of this dissociation barrier on low-index Cu surfaces has been experimentally determined to be 3–5 kcal/mol by H_2 scattering experiments.[10] Measuring the desorption velocity and angular profile of hydrogen after bulk permeation, Comsa and David[11] find an even larger barrier, which might be due to a subsurface state leading directly to desorption.

The binding of hydrogen atoms to transition-metal surfaces is theoretically quite well understood.[12–17] The nature of the dissociation mechanism, on the other hand, is not quite as clear, especially with respect to the involvement of the substrate d electrons.[18–21] The picture presented by Melius *et al.*[18] involves symmetry changes in the total wave function between s and d electrons, but leaves the total occupation of the d levels unchanged. Siegbahn *et al.*[19] calculate that the dissociation barrier is increased by 50 kcal/mol if the d electrons at the dissociation site are not included in the interaction. On the other hand, Harris and Andersson[20] propose a model where the interaction between H_2 molecule and the surface is through the sp electrons, but this interaction is facilitated by a change in sd hybridization at the surface, which

changes the nominal d occupancy. This picture is consistent with the "chemical approach" presented by Upton.[21] Here a large density of unoccupied states immediately near E_F allows the substrate orbitals to adjust to the approaching molecule and maximize bonding interaction, while minimizing repulsion due to Pauli exclusion.

To study the nature of the dissociation barrier for H_2 chemisorption we have determined the electronic structure of epitaxially grown Ni overlayers on Cu as well as ordered Cu films on Ni and then exposed these films to hydrogen. In contrast to a bare Cu crystal, a monolayer of epitaxially grown Ni on Cu exhibits unoccupied d states at the Fermi level localized at the metal-vacuum interface. Vice versa, a Cu monolayer (ML) on Ni "covers" the d holes of the Ni substrate. We have chosen the Ni/Cu(111) system since nickel grows pseudomorphically on the Cu(111) surface up to 7 ML.[22,23] This behavior might be expected from the small lattice mismatch of 2.5% between Ni and Cu. Angle-resolved ultraviolet photoemission spectroscopy (ARUPS) and k-resolved inverse photoemission spectroscopy (KRIPES) have been applied to investigate the electronic structure of monolayer Ni films on Cu(111) and the changes upon hydrogen adsorption. The bare Cu substrate has been extensively studied by ARUPS (Ref. 24) and KRIPES (Ref. 25). Observation of the Ni-induced features is facilitated by a projected bulk band gap at $\bar{\Gamma}$ of the surface Brillouin zone of the Cu(111) substrate which includes the Fermi level E_F. In this energy range near E_F the two-dimensional Ni bands might be expected from a tight-binding calculation by Tersoff and Falicov[3] and a previous photoemission study by Kirstein *et al.*[2] on the Ni/Cu(111) system. Only the *sp*-derived Λ_1 intrinsic Cu(111) surface state 0.39 eV below E_F at $\bar{\Gamma}$ (Ref. 26) might interfere with the Ni-overlayer bands.

In Sec. II we describe the experimental procedure, while in Sec. III we report the experimental results. In Sec. III A the electronic structure of the Ni/Cu(111) system will be presented and discussed. In Sec. III B the changes of the electronic structure upon hydrogen adsorption will be demonstrated and compared to hydrogen adsorption in the bare Ni(111) crystal. Conclusions will be drawn in Sec. IV.

II. EXPERIMENT

The angle-resolved photoemission experiments were carried out using a 50-mm hemispherical analyzer with $\pm 1°$ angular acceptance (VSW) and synchrotron radiation from the BESSY storage ring using the TGM-3 beamline. The total-energy resolution was 200 meV (0.3 eV) at a photon energy of 14 eV (40 eV), where most of our data were taken. The experimental setup is described in more detail in the literature.[27] The KRIPES experiments were performed in a separate ultrahigh-vacuum chamber. The inverse photoemission measurements were performed in the isochromat mode, detecting 9.5-eV photons with a Geiger-Müller–type counter filled with iodine as a detecting gas and a SrF_2 window. The photon acceptance angle was fixed at $70° \pm 15°$. The electrostatically focused electron gun with a BaO cathode was mounted on a two-axis goniometer allowing for a change of electron incidence angle. The electron-beam divergence was 3°, resulting in $\Delta k_{\parallel} = 0.06$ Å^{-1}. The overall energy resolution (electron source plus photon detector) was 350 meV.

The Cu(111) crystal was cleaned by argon-ion sputtering and subsequent annealing. Cleanliness was checked by Auger-electron-spectroscopy (AES), KRIPES, and ARUPS measurements. Nickel has been evaporated from a resistively heated W-filament wrapped with Ni wire. Due to the careful out-gassing of the Ni oven and the application of a water-cooled shield, the pressure increase (base pressure 1×10^{-10} mbar) during evaporation could be limited to 3×10^{-10} mbar. During deposition the sample temperature was held at about 180 °C. This temperature is a compromise in order to obtain pseudomorphic well-ordered overlayers and to avoid interdiffusion of nickel and copper.[22] Using this evaporation condition, Tear and Roll[28] have observed no or very little alloying of the surface layer from low-energy electron diffraction (LEED) (IV) studies. In fact, the ordering of the Ni surface layer could be verified by a perfect (1×1) LEED pattern. Nickel evaporation onto the Cu(111) substrate at room temperature exhibits relatively diffuse LEED spots. However, a distinct improvement could be achieved by subsequent annealing of the films deposited at room temperature. Concomitantly, the amplitude of the $n = 1$ image-potential surface-state feature in the KRIPES spectra (see below) increased by a factor of 2 and its width is narrowed by about 30%. We attribute both observations to the ordering of the Ni overlayer.

In the series of the KRIPES experiments the film thickness was monitored by AES, which is complicated

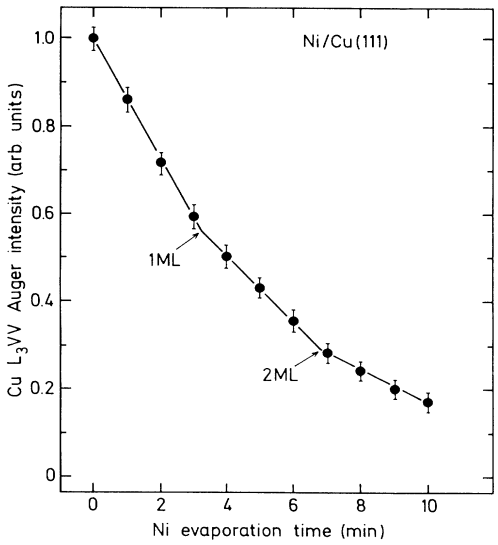

FIG. 1. Intensity of the Cu L_3VV Auger transition at 920 eV as a function of Ni evaporation time. This substrate transition is not superimposed by a Ni emission line. The evaporation source has been held at constant temperature. Completion of the first and second Ni layer is indicated by the distinct changes of slopes.

due to the close similarity of the copper and nickel Auger spectra. Following the procedure as outlined in Ref. 28, we have compared the Cu L_3VV Auger line with the intensity of the superposed Ni L_3VV, Cu $L_3M_2,M_{2,3}$ transitions. The Cu L_3VV line at 920 eV does not overlap with a Ni feature. If the Ni evaporation rate is constant, its intensity-versus-evaporation time curve exhibits straight lines with different slopes provided that the Ni grows layer by layer on Cu(111). The bends are characteristic for the completion of a monolayer in the layer-by-layer growth of the Ni film.[2] This functional dependence has been observed experimentally, as plotted in Fig. 1. It clearly demonstrates the completion of the first and second Ni layer, respectively. We have used these results to calibrate the Ni monolayer coverage. The estimated error is about 10% for the monolayer Ni coverages presented in this paper. For the ARUPS experiments, film thicknesses have been monitored by a microbalance which was checked against the intensity ratios of the Ni and Cu $3p$ core levels excited with $h\nu=150$ eV photon energy at the synchroton. Again, an error bar of 10% can be given.

III. RESULTS AND DISCUSSIONS

A. Electronic structure of 1-Ni-ML Ni(1×1)/Cu(111)

Figure 2 shows the normal-incidence inverse photoemission spectra taken for clean Cu(111) and a 1-ML

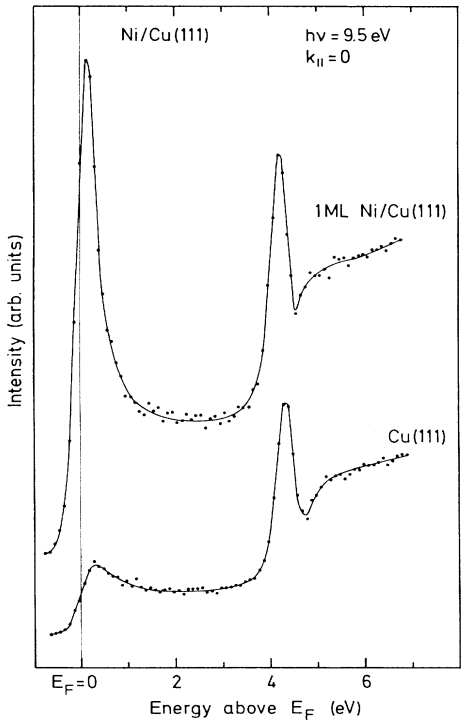

FIG. 2. Isochromat inverse photoemission spectra from Cu(111) (bottom) and 1 ML of Ni(1×1)/Cu(111) (top) taken at normal electron incidence. The solid lines are drawn to guide the eye.

pseudomorphic Ni overlayer on Cu(111). Both curves in Fig. 1 are normalized to the absorbed current and shown on the same scale. The KRIPES spectrum from the bare Cu(111) surface has been reported previously[25] and our spectrum shows the same structures as the published one. It is dominated by a narrow peak [0.35 eV full width at half maximum (FWHM)] at 4.25 eV above E_F. This peak is located 0.7 eV below the vacuum level $E_{\rm vac}$ [$\phi_{\rm Cu(111)}=4.94$ eV (Ref. 29)] and has been attributed to the fundamental $n=1$ image-potential surface state.[25] Higher series members ($n=2,3,\ldots,\infty$) converge towards the vacuum level, giving rise to the steplike feature at 4.8 eV. We attribute the small peak at E_F to the *sp*-derived intrinsic surface state,[26] 0.39 eV *below* E_F at Γ. This feature is only visible due to the finite energy and momentum resolution of the KRIPES spectrometer.

Deposition of 1 ML of Ni atoms gives rise to a large peak at E_F in the IPES spectrum for normal-incidence electrons. We ascribe this narrow feature to Ni d-derived holes in contrast to band-structure calculations by Tersoff and Falicov,[3] which predict holes in the topmost d band of the Ni monolayer on Cu(111) only near the boundary of the surface Brillouin zone (SBZ). The image-potential states are still visible at $E_F+4.15$ eV, with the same line shape as on the bare Cu(111) surface. As mentioned above, the narrow linewidth indicates a highly ordered Ni overlayer giving rise to a well-defined SBZ and $\bar{\Gamma}$ point, respectively. The $n=1$ binding energy with respect to $E_{\rm vac}$ is very similar for both systems since the work function of the ML Ni(1×1)/Cu(111) system is reduced by $\Delta\phi-0.15$ eV with respect to the clean Cu(111) surface. This decrease is rather unexpected since the work function of the bare Ni(111) surface is larger than for the Cu(111) substrate. The explanation for that observation is not yet clear. A similar work-function reduction for Pd/Al(111) has been related to the difference of the surface electronic structure of the Pd monolayer on Al(111) and the bare Pd(111) surface.[30] These are minor changes which have to be expected for this pseudomorphic metal-on-metal overlayer. The extra atomic layer shifts the terminating plane of the crystal as well as the image-potential reference plane outwards. The L_2'-L_1 band gap and, therefore, the projected bulk band gap at $\bar{\Gamma}$ should be mainly unaffected by the Ni monolayer, even if the two-dimensional Ni-derived bands near the Fermi level E_F modify the bottom of the projected gap to some extent. Going from the 1-ML Ni(1×1)/Cu(111) system to a bare Ni(111) surface, the gap and the vacuum level change. The $n=1$ image-potential state would then be located at 4.6 eV above E_F.[31]

We have also measured the *occupied electronic states using angle-resolved* photoemission. The normal-emission spectra of clean Cu(111) and 1- and 1.5-ML nickel on the Cu(111) substrate are shown in Fig. 3. The energy-distribution curves (EDC's) shown are taken at two different photon energies: $h\nu=14$ and 40 eV. The *sp*-derived Λ_1 intrinsic surface state -0.39 eV below E_F in the $L_{2'}$-L_1 gap of Cu(111) (Ref. 26) exhibits a cross-section minimum at about $h\nu=40$ eV.[32] This is reflected in the spectra in Fig. 3. We have used this cross-section

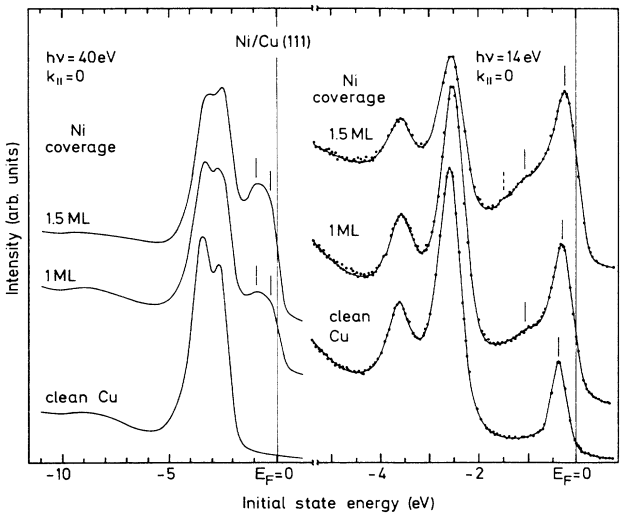

FIG. 3. Normal-emission photoemission spectra from Cu(111), 1 ML Ni(1×1)/Cu(111), and 1.5 ML Ni/Cu(111) at 14 eV (right-hand panel) and 40 eV (left-hand panel) photon energy.

effect to separate the contributions from the remaining part of the intrinsic Λ_1 Cu(111) surface state and the "new" Ni-induced bands. The peaks at binding energies below 2 eV have been attributed to bulk transitions from $\Gamma_{12}-\Lambda_3-L_3$ and $\Gamma_{25'}-\Lambda_1-L_{2'}$ bands, respectively.[24] A full Ni monolayer evaporated on Cu(111) induces a significant increase of emission in the binding-energy range between E_F and -2 eV. At $E_B=-1.1$ eV a well-pronounced peak shows up in the spectrum taken with $h\nu=40$ eV. In addition, a weak shoulder has been discernible at -0.3 eV. This band is clearly discernible at -0.3 eV in the normal-emission spectrum excited by 14 eV photon energy. We will discuss below in more detail this assignment and the relationship to the intrinsic Λ_1 surface state on Cu(111). The second band has been identified again as the small feature at -1.1 eV binding energy. Furthermore, a very weak feature can be identified at -1.4 eV binding energy in the 1.5-ML spectrum. The main features shifts slightly towards E_F with increasing Ni coverage (see Fig. 3). The intrinsic surface state seems to persist through the deposition of a Ni monolayer. In the 1-ML spectrum (14 eV) the Λ_1 surface-state emission is still visible as a shoulder at the high-energy side of the main feature at -0.3 eV.

Due to the superposition of the Ni-derived features in the ARUPS spectrum the existence of the Λ_1 state as an interface state of the Ni(1×1)/Cu(111) system has to be proven independently. This has been done by a KRIPES study of the ML Ni(1×1)/Cu(111) system. In Fig. 4, KRIPES spectra are shown taken as a function of electron incidence angle θ along the $\bar{\Gamma}\bar{K}$ azimuth of the SBZ. On the top, near-normal-incidence spectra at $-2.5°$ and 2.5° are plotted. Slight differences in relative peak intensities with respect to the spectrum in Fig. 2 are mainly caused by the small differences in the preparations of the ML. Away from normal incidence the intensity of the feature at the Fermi level increases by a factor of 2 for $\theta=0.75°$ and 2.2 for $\theta-12.5°$. At $\theta=17.5°$ the spectrum exhibits a double-peak structure at 0.3 and 0.7 eV above E_F. Increasing the electron incidence angle further, the higher-lying peak disperses to 1.5 and 2.2 eV, respectively. In contrast, the Ni-derived band seems to cross below E_F at $\theta\geq 22.5°$. These measurements clearly demonstrate the Fermi-level crossing of the Λ_1 surface state.

In Fig. 5 the two-dimensional dispersion relations $E(k_\parallel)$ of the dispersing features of Fig. 4 have been plotted measured along $\bar{\Gamma}\bar{K}$. For comparison, KRIPES results are shown for the bare Cu(111) surface along both high symmetric azimuths. The dispersion of the Λ_1 surface state on Cu(111) has been added as determined along $\bar{\Gamma}\bar{M}$ by high-resolution ARUPS measurements by Kevan.[26] He fits a parabola with an effective electron mass of $m^*=0.46m_e$ to the dispersion curve, which has been extended above the Fermi level in Fig. 5. There is a remarkably good correspondence with the KRIPES measurements at the crossover point. Only at $k_\parallel>0.5$ Å^{-1} does a deviation become visible, where the unoccupied surface state leaves the projected bulk band gap. It

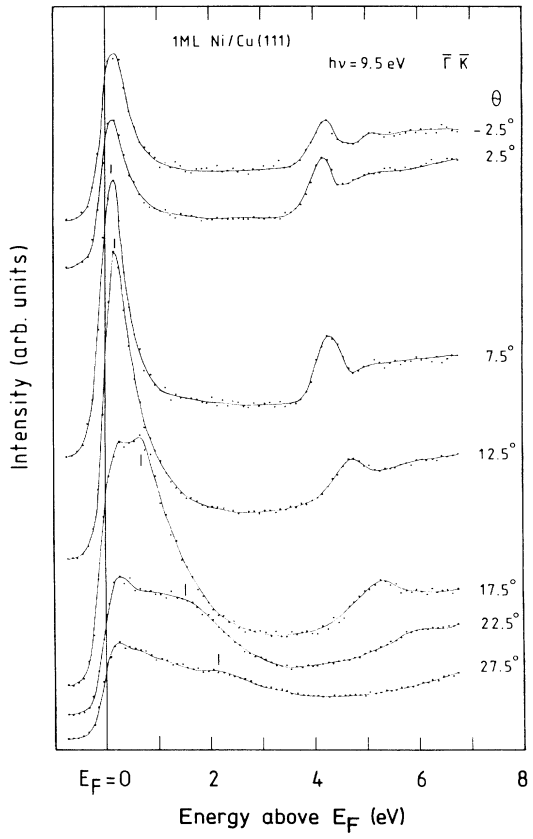

FIG. 4. Isochromat inverse photoemission spectra from 1 ML Ni(1×1)/Cu(111) for electrons incident at various polar angles θ in the $\bar{\Gamma}\bar{K}$ azimuth of the SBZ. The marks indicate the dispersion of the Λ_1 intrinsic surface state of the Cu(111) substrate.

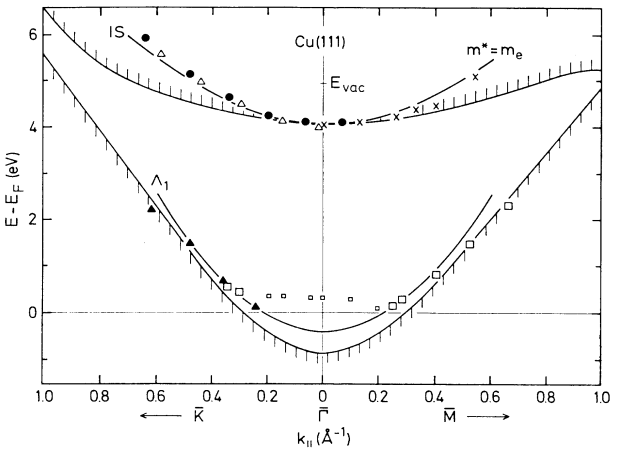

FIG. 5. Experimental $E(k_{\parallel})$ dispersion relations of the unoccupied states for clean Cu(111) and for 1 ML Ni(1×1) on Cu(111). The electrons were incident along the $\bar{\Gamma}\bar{K}$ and $\bar{\Gamma}\bar{M}$ azimuth, respectively. Unshaded areas indicate the gap of the projected bulk band structure. Open squares represent our experimental results for the Λ_1 surface state dispersion, crosses show the dispersion of the fundamental $n=1$ image state (IS), and open triangles depict the measurements of Hulbert *et al.* (Ref. 25) along $\bar{\Gamma}\bar{K}$ for the bare Cu(111) surface. The image state can be described by a free-electron ($m^*=m_e$) dispersion. The Λ_1 surface state closely follows the $m^*=0.46m_e$ parabola (solid line) determined by Kevan (Ref. 26) from the occupied part of the Λ_1 band. ▲ and ● represent our experimental results for the Λ_1 surface state and the IS state, respectively, from the 1-ML Ni(1×1)/Cu(111) sample. Note that both surface-state bands are unaffected by the Ni adsorption.

should be noted here that our KRIPES results are in very good agreement with previous inverse photoemission studies.[25] The data points at about 0.2 eV above E_F around $\bar{\Gamma}$ are due to the limited energy and $k_{\parallel}$ resolution. These features in the KRIPES spectra of the *clean* Cu(111) surface are about a factor of 10 smaller than the full Λ_1 signal at $k_{\parallel}=0.3$ Å^{-1}. In spite of the fact that Kevan's measurements have been done along the $\bar{\Gamma}\bar{M}$ azimuth, we have used the same $E(k_{\parallel})$ parabola for the $\bar{\Gamma}\bar{K}$ direction as a reasonable approximation supported by our KRIPES measurement (see Fig. 5) and by the results of Hulbert *et al.*[25] Concerning the pseudomorphic Ni monolayer on Cu(111), the dispersion of the prominent feature crossing the Fermi level at about 0.23 Å^{-1} fits the extended Λ_1 dispersion, very well demonstrating the persistence of this intrinsic Cu(111) surface state as an interlayer state. Since the dispersion is unchanged, the Λ_1 state seems to be unaffected by the Ni overlayer, keeping the band minimum at −0.4 eV below E_F.

This important observation substantiates our interpretation of the peak seen in the KRIPES spectrum at $\bar{\Gamma}$. This peak is due to *d* holes and not caused by the Cu surface state shifted above E_F. Since the dispersion of the Λ_1 interface state matches the dispersion of the intrinsic surface state, the shift of the photoemission peak in Fig. 2 at $h\nu=14$ eV with Ni coverage has to be due to additional emission from the Ni overlayer bands. Together with the shoulder observed at $h\nu=40$ eV at 0.3 eV this supports the assignment of an occupied Ni band at −0.3 eV at $\bar{\Gamma}$. It is worthwhile to note at this point that the Ni(111) surface exhibits the analogous Λ_1 surface state as Cu(111) in the same region of energy-momentum space.[33] However, this state disperses downwards from E_F and does not cross the Fermi level. Judging from the calculated[3] dispersion for the highest-energy band of the Ni overlayer and by analogy to bulk Ni, this band is of a symmetry that does not interfere with the existence of a Λ_1 surface state, whereas the band at −1.1 to −1.4 eV should have the same symmetry (d_{z^2} or sp_z). In addition, the latter bands are situated outside the projected bulk band gap below the $L_{2'}$ point at −0.9 eV binding energy.

As mentioned before, the $n=1$ image-potential surface state is preserved on the ML Ni/Cu(111) system. Furthermore, its dispersion has not been influenced. In Fig. 5 this experimental $E(k_{\parallel})$ relation is compared to the KRIPES results of Hulbert *et al.*[25] for the clean Cu(111) surface. Both dispersions can be well described by the same free-electron parabola with an effective electron mass of $m^*=1m_e$ (see Fig. 5), in excellent accord with a recent two-photon photoemission study by Kubiak.[34] Obviously, the modification of the Cu(111) surface by a Ni monolayer neither changes the *sp*-inverted $L_{2'}$-L_1 bulk band gap nor the surface barrier. Both the width of the gap and the image-potential form of the barrier potential have been successfully applied to describe the intrinsic and image-potential surface states in a one-dimensional multiple-reflection model.[35–37]

At this point we will return to the Ni-induced electronic structure and first try to reconcile our observations with the calculated band structure for a monolayer Ni film on Cu(111).[3] These calculations predict that the monolayer Ni film on Cu(111) is magnetically "dead," i.e., the magnetic exchange splitting of the bands is calculated to be 0.1 eV or less. This would result in only two degenerate bands at the center of the SBZ, at −0.37 and −1.41 eV.[3] As mentioned above, no hole states immediately above E_F should be observed at $\bar{\Gamma}$ either. Our data, on the other hand, indicate that this film is magnetic and that the exchange splitting pushes the minority band above E_F near the $\bar{\Gamma}$ point of the SBZ, which accounts for the hole states we see in the KRIPES spectra 0.1 eV above E_F. Obviously, this also explains the observation of three different occupied bands at $\bar{\Gamma}$, about where we observe structures at −0.3, −1.1, and a very weak one at −1.4 eV in the angle-resolved photoemission spectra. This situation would be rather similar to bulk Ni, where the Λ_3 minority band has a small hole pocket near the *L* point.[33,34] In summary, we attribute the Ni *d* states at −0.3 and +0.1 eV to majority- and minority-spin bands, respectively, separated by an exchange splitting of 0.4 eV, while the lower bands exhibit an exchange splitting of 0.3 eV. This result is comparable to a magnetic monolayer of nickel on Cu(100), where an exchange, splitting of 0.3 eV has been found experimentally by ARUPS measurements[1] in accordance with slab calculations.[3,4]

Earlier experimental results on the magnetism of thin

Ni films either are in agreement[38] or disagreement[39] with our results. However, in these early studies the films were not well characterized with respect to their order. Especially in the studies of Bergmann,[39] the films were evaporated onto a target held at a temperature of 10 K, which does not yield an ordered film. However, a definite determination of the spin character of the two-dimensional bands of the Ni/Cu(111) system has to await spin-resolved ARUPS and KRIPES measurements, respectively.

B. H_2 chemisorption on a Ni monolayer on Cu(111)

Having established the details of the electronic structure of the Cu(111) surface modified by a monolayer of Ni atoms, we now want to discuss hydrogen dissociation and chemisorption. In Fig. 6 the ARUPS spectra of a complete monolayer Ni and 1.5-ML Ni are shown at 40 and 14 eV photon energy, respectively. They are compared with the spectra obtained after saturation of the surface with hydrogen, which has been achieved by an exposure of 10 L H_2 (1 L = langmuir $=10^{-6}$ torr s) with the sample at a temperature of about 140 K. A slight increase of the work function of $\Delta\phi=50$ meV has been measured after hydrogen adsorption. This value, however, is just at the detection limit of the diode method used to measure the work-function changes in these experiments. Saturation with hydrogen has very little effect on the 40-eV spectrum. The intensity of the band directly below E_F is reduced. This effect is much more evident in the 14-eV spectrum in the right-hand panel of Fig. 6. Here the Ni-derived band at -0.3 eV is almost completely quenched. The Λ_1 surface state of the Cu(111) substrate (or interface state) emerges again at -0.4 eV obviously not affected by the hydrogen. In agreement with the 40-eV spectrum, the transitions at -1.4 and -1.1 eV are less influenced.

The left-hand panel of Fig. 7 shows the isochromat spectrum of the clean ML Ni/Cu(111) sample as well as the spectrum after 10 L H_2 exposure. The $n=1$ image-potential surface state is reduced in intensity and slightly shifted by 0.1 eV towards the Fermi level. The Ni-derived peak at E_F, however, exhibits a substantial reduction. A short flash to about 150 °C desorbs the hydrogen again, as deduced from the restored KRIPES spectrum (see Fig. 7). The analogous behavior has been observed for the hydrogen chemisorption on a bare Ni(111) surface. In the right-hand panel of Fig. 7 the KRIPES spectrum of the clean Ni(111) surface is plotted. Note the $n=1$ image-potential surface state at 4.6 eV and the Ni d holes directly at the Fermi level. An exposure of 10 L hydrogen at about 140 K induces a similar reduction of the amplitudes of the Ni d holes as well as the image state. Yet at $E_F+1.7$ eV a new state has been developed clearly visible in the KRIPES spectrum in Fig. 7. We attribute this feature on the Ni(111) surface to the unoccupied *antibonding* counterpart of the bonding hydrogen level split off from the Ni d bands. Saturation coverage on Ni(111) has been checked by changing the hydrogen exposure between 5, 10, and 20 L. No changes have been observed either in the amplitude of the hydrogen-induced state nor in its energy position. For a complete (1×1) overlayer of atomic hydrogen on Ni(111), the *bonding* split-off band has been previously found at -9.0 eV at $\bar{\Gamma}$ by ARUPS.[8] A bandwidth of 3.2 eV along $\bar{\Gamma}\bar{M}$ and 4.2 eV along $\bar{\Gamma}\bar{K}$, respectively, has been determined[8] for this two-dimensional state in a gap of the projected bulk band structure. The antibonding H $1s$ – Ni d band 1.7 eV

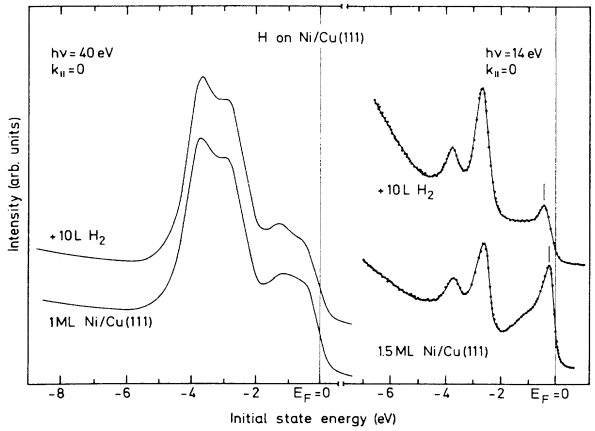

FIG. 6. Normal-emission photoemission spectra (14 and 40 eV photon energy) from 1 and 1.5 ML Ni(1×1)Cu(11) and after exposure of both samples to 10 L H_2 at about 140 K.

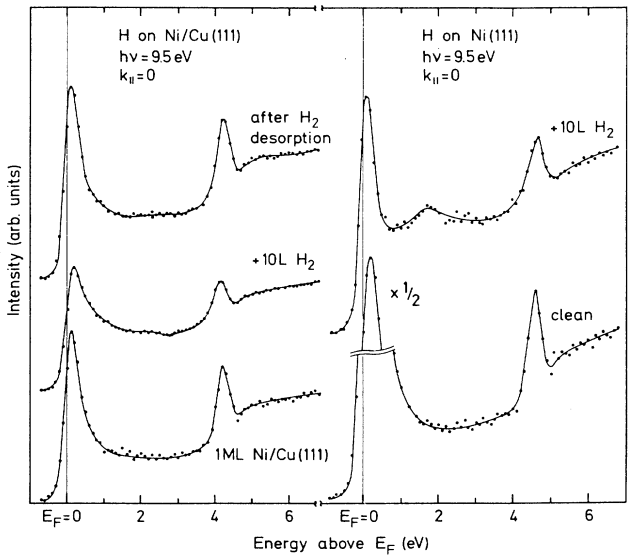

FIG. 7. Isochromat inverse photoemission spectra taken at normal electron incidence. In the right-hand panel the spectrum of clean Ni(111) is compared to the spectrum after exposure to 10 L H_2 at 140 K. Note the antibonding split-off state at 1.7 eV above E_F (see text). In the left-hand panel the spectrum from the 1-ML Ni(1×1)/Cu(111) surface is compared with the spectra of this composite surface exposed to 10 L H_2 ($T\simeq140$ K). Hydrogen desorption after a short flash to about 150 °C is indicated by the recovered KRIPES spectrum on the top left-hand side of the figure.

above E_F at $\bar{\Gamma}$ is also located within a projected bulk band gap of the Ni(111) surface. Therefore, it is clearly separated from Ni bulk band features in the KRIPES spectrum of Fig. 7.

The energy of the antibonding hydrogen-induced state is in reasonable correspondence with cluster calculations[13,40] which predict a Ni d state shifted above E_F due to interaction with the H 1s orbital. Good agreement has been found with calculations of Newns,[41] who used the Anderson formalism in a Hartree-Fock approximation neglecting the H 1s interaction with the Ni sp band. He finds the antibonding H 1s–Ni state at 2 eV above E_F, in agreement with Anderson-model calculations by Schönhammer, who included the Ni sp bands.[42] However, both calculations are based on an incorrect experimental binding energy of -5.8 eV for the *bonding* state (see Ref. 8). Considering the actual energy of the split-off band,[8] corrections for the antibonding level have to be expected. In addition, the H 1s–derived resonance of the negative-ion final state has been determined at 2 eV above E_F using a modified Anderson mode.[43] It should be added here that Reimer *et al.*[44] have observed an unoccupied H-induced level 1.3 eV above E_F from angle-integrated inverse photoemission studies on the H/Ni(100) system. The energy difference might be caused by the method they used to identify the antibonding state, namely subtraction of the clean IPE spectrum from the hydrogen-covered one.

Preliminary results on the angular dependence of the antibonding band of H/Ni(111) exhibit a negligible dispersion up to a wave vector of $k_{11}=0.2$ Å^{-1} taken along the $\bar{\Gamma}\bar{M}$ azimuth. Simultaneously, a decrease of the H-induced signal in the KRIPES spectra has been found. Due to the limited data set, we have to attribute this observation either to considerable disorder and/or the merging of the empty split-off state into the bulk bands at higher k_{11} values. However, further experiments are necessary since we expect a similar dispersion of the empty band as has been measured for the bonding split-off band of H/Ni(111) as well as H/Pd(111).[8]

Having discussed the hydrogen adsorption on the bare Ni(111) surface, we return to the interaction of H_2 with the pseudomorphic Ni(1×1)/Cu(111) substrate. In addition to the reduction of the amplitude of the Ni-induced features in the KRIPES spectrum of the hydrogen-covered system (see Fig. 7, left-hand panel), a small structure can be identified at 2 eV above E_F. By comparison to the H/Ni(111) system, we attribute this weak feature to the antibonding split-off state. The small amplitude might be explained by a lower sticking coefficient of hydrogen on the Ni(1×1)/Cu(111) system at 140 K, resulting in a smaller hydrogen coverage.

The small feature 2 eV above E_F in the KRIPES spectrum of Fig. 7 is so far the only hydrogen-induced state we could identify on the composite surface, yet hydrogen absorption is clearly evident by the considerable decrease of spectral intensities of the Ni derived d holes and the occupied state at -0.3 eV below E_F (see Figs. 6 and 7). Part of that decrease might be explained by inelastic scattering at the adsorbed hydrogen species. However, we attribute these changes mainly to a real reduction of the surface density of states of the two-dimensional Ni-derived d states upon bonding to hydrogen. A similar removal of intrinsic surface states or resonances from the energy region at E_F has been previously detected by an ARUPS experiment on H/Ni(111).[8,45]

In conclusion, ARUPS and KRIPES measurements demonstrate that molecular hydrogen *dissociates* at the 1-ML Ni(1×1)/Cu(111) surface, while it does not on bare Cu(111).[9] The main difference between the clean Cu(111) surface and the modified surface is the existence of d states directly at the Fermi level, especially a small pocket of d holes located at $\bar{\Gamma}$ in the SBZ. Intuitively, this observation seems like a direct confirmation of the model presented by Harris and Andersson.[20] However, we have to add here that we do not "see" the actual dissociation process. We only observe that the chemical bonding of hydrogen atoms changes the d holes. On the other hand, without the d holes the dissociation does not occur.

Even though the peak in the IPES spectrum showing the d holes is quite large, the total density of states near the Fermi level is not changed by a large amount on the modified surface. The d holes only occupy a very small portion of momentum space. Therefore we believe that the reduction of the dissociation barrier is not due to a general increase in the density of states at E_F, but rather to the specific quality of d holes. This allows the sp electrons to be more flexible and to react to the approaching H_2 molecule by changing the degree of s-d hybridization.

Finally, we are able to demonstrate experimentally that the empty d states have to be located directly at the surface to dissociate the H_2 molecule. In Fig. 8 the normal-incidence KRIPES spectra have been displayed for clean Ni(111) and a monolayer of Cu on Ni(111). Like nickel on Cu(111), copper grows pseudomorphically on a Ni(111) substrate. The monolayer coverage has been controlled by AES and a good (1×1) LEED pattern has been observed. The work function decreases by $\Delta\phi=-0.2$ eV. The spectrum of Fig. 8 exhibits no extra unoccupied features at $\bar{\Gamma}$. The intensity of the d-hole feature of the underlying Ni(111) surface is slightly decreased due to the finite mean free path of the impinging electrons. The $n=1$ image-potential surface state shifts to lower energies since it is fixed to the vacuum level. Exposure of the 1-ML Cu(1×1)/Ni(111) surface at 140 K to 10 L H_2 does not change the KRIPES spectrum on the top of Fig. 8. The slight decrease in intensity of less than 10% is within the experimental error bar. Therefore we conclude that one layer of pseudomorphically grown Cu atoms on the Ni(111) surface "covers" the Ni d holes. They are localized below the topmost Cu-vacuum interface. Therefore they are not available for the dissociation. In this process the Pauli repulsion is reduced by $s\rightarrow d$ transfer of metal s electrons to avoid the energy cost of penetrating the H_2 $1\sigma_g$ bonding orbital.[20] Obviously, the function of the metal d holes as a sink for the s electrons is confined to the outermost metal layer. On the 1-ML Cu(1×1)/Ni(111) surface, Cu d-states are occupied. Accordingly, the entrance-channel activation barrier cannot be lowered by $s\rightarrow d$ charge transfer and H_2 is not dissociated.

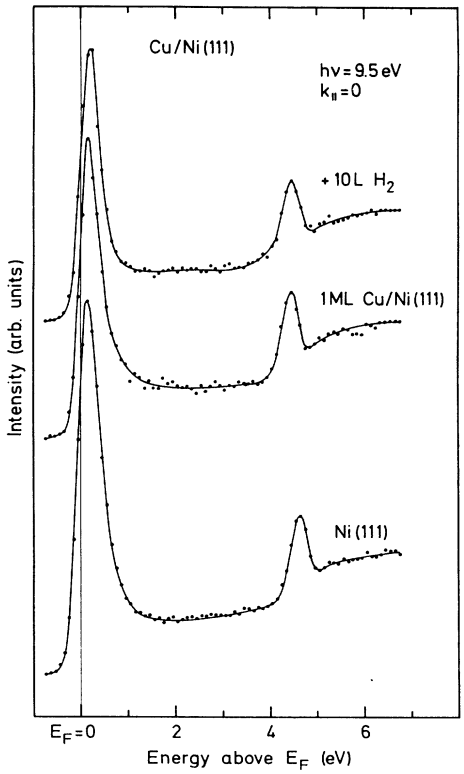

FIG. 8. Normal-incidence isochromat inverse photoemission spectra of Ni(111) and 1 ML Cu(1×1)Ni/(111). On the top the spectrum after exposure of the 1 ML of Cu atoms adsorbed on Ni(111) to 10 L molecular hydrogen at about 140 K.

IV. CONCLUSIONS

By angle-resolved inverse photoemission and photoemission spectroscopy we have studied the electronic structure of a pseudomorphic monolayer of Ni atoms on a Cu(111) surface. At the $\bar{\Gamma}$ point of the SBZ three different Ni-derived bands have been found at 0.1 eV above the Fermi level and at −0.3 eV, as well as −1.1 eV below the Fermi level. In addition, we observe a weak fourth band at −1.4 eV. These findings are in contrast to a tight-binding band-structure calculation[3] for a nickel monolayer on Cu(111) which predicts majority-spin bands at −0.37 and −1.41 eV below E_F at $\bar{\Gamma}$. The minority bands are found at about 0.1 eV less binding energies.[3] However, we attribute the Ni d-derived bands at 0.1 and −0.3 eV to minority- and majority-spin bands separated by an exchange splitting of 0.4 eV. The low-lying bands at −1.1 and −1.4 eV exhibit an exchange splitting of 0.3 eV. Therefore the Ni monolayer on Cu(111) is magnetic, in contradiction to the above-mentioned calculations which predict a magnetically "dead" layer. Spin-resolved ARUPS and KRIPES measurements on that system are clearly necessary to clarify the spin character of the various observed bands.

The Λ_1 intrinsic surface state of the Cu(111) substrate persists during the Ni-monolayer adsorption and remains localized at the Cu-Ni interface. Neither the bottom of this two-dimensional band −0.4 eV below E_F at $\bar{\Gamma}$ nor its dispersion along $\bar{\Gamma}\bar{K}$ of the SBZ has been affected by the Ni overlayer. As judged from the calculations of Tersoff and Falicov,[3] the symmetry of the highest Ni-derived bands does not interfere with the Λ_1 surface-state band. The lower bands at −1.1 and −1.4 eV have the same symmetry (d_{z^2} or sp_z), yet they are located below the $L_{2'}$-L_1 bulk band gap of the Cu(111) substrate. We attribute these reasons to be responsible that the projected bulk band gap and necessarily the Λ_1 surface state is not distorted by the Ni monolayer on the Cu(111) crystal. Furthermore, the surface barrier of the composite Ni/Cu(111) system has not been changed. Only the reference plane of the image potential is displaced outwards by the addition of the metallic Ni layer on the Cu(111) metal, yet the binding energy and the dispersion of the fundamental $n=1$ image-potential surface state are unaffected. A binding energy of 0.7 eV with respect to the vacuum level and a free-electron-like dispersion ($m^*=m_e$) has been observed for the bare and the Ni-covered Cu(111) surface.

The main difference of the electronic structure between the Cu(111) substrate and the composite monolayer Ni(1×1)/Cu(111) system is the existence of a local density of d-derived states at the Fermi level. This seems to be the most crucial parameter that governs the dissociation process of molecular hydrogen at transition-metal surfaces.[20] Therefore we have exposed the Ni/Cu(111) system, the bare Ni(111) surface, and the pseudomorphically grown 1-ML Cu(1×1)/Ni(111) surface to molecular hydrogen at sample temperatures of about 140 K. The normal-incidence KRIPES spectrum of a 10-L H_2 dosage on Ni(111) exhibits a well-pronounced antibonding split-off state at 1.7 eV above E_F. This is the first unique determination of the counterpart of the bonding hydrogen level split off from the Ni d bands.[8] The energy of this unoccupied (H 1s–Ni d)-derived state is in good agreement with various calculations using the Anderson-Newns formalism[41,42] as well as cluster models.[13,40] The direct confirmation of the atomic hydrogen chemisorption is accompanied by a considerable reduction of the intensity of the d-hole feature in the KRIPES spectrum. ARUPS as well as KRIPES spectra of the hydrogen-exposed Ni/Cu(111) surface clearly prove the adsorption of hydrogen. The Ni d-derived band at −0.3 eV as well as the d holes 0.1 eV above E_F show a considerable decrease in spectral intensity. The antibonding split-off band is also visible in the KRIPES spectrum at about 2 eV, yet its intensity is very small and is attributed to a small hydrogen sticking coefficient on the Ni/Cu(111) surface. In contrast to this, hydrogen is not dissociated on the 1-ML Cu(1×1)/Ni(111) surface. The KRIPES spectrum of this system exhibits no change upon hydrogen exposure. From our photoemissions studies we also conclude that molecular hydrogen is dissociated on a monolayer of Ni/Cu(111), while it does not dissociate on 1-ML Cu/Ni(111), just as on a bare Cu(111) surface.[9] We have to add that photoemission is not able to "see" the dynamical dissociation process, yet we observe its results, namely whether hydrogen is adsorbed or not.

Our experiments support the model presented by

Harris and Andersson.[20] Here the d holes at the Fermi level serve as sinks for the transition-metal s electrons spilling out into vacuum. These s electrons must orthogonalize with respect to the bonding σ_g orbital of the approaching H_2 molecule, shifting these s electrons up in energy, leading to a considerable activation barrier. If d holes are available at E_F, an $s \rightarrow d$ charge transfer avoids the energy increase. As a result, the activation barrier is practically zero for transition metals such as Ni, Pt, and Nd. However, this process is highly localized at the outermost layer, as deduced from the Cu/Ni(111) system. We ascribe the nondissociative property of a monolayer of Cu/Ni(111) to the covering of the underlying Ni d holes at E_F by the Cu overlayer.

In summary, our angle-resolved photoemission and inverse photoemission experiments demonstrate how the modification of the surface electronic structure of Cu(111) by a monolayer of pseudomorphically grown nickel, and, vice versa, of Ni(111) by a pseudomorphic monolayer of copper, influences the hydrogen chemisorption properties of the bare transition-metal surfaces.

ACKNOWLEDGMENTS

The authors want to acknowledge valuable discussions with K. Jacobi and E. E. Koch, and thank M. L. Miranda-Rocco for help with the measurements. We especially thank K. Jacobi, who made available to us his evaporation sources. One of us (W.E.) would like to thank the BESSY staff for their hospitality. This work was supported in part by the Bundesministerium für Forschung und Technologie (BMFT) for funds for research with synchrotron radiation (Contract No. 06 390 FX9/C3-09).

*Permanent address: Exxon Research and Engineering Company, Route 22 East, Annandale, NJ 08801.

[1]M. A. Thompson and J. L. Erskine, Phys. Rev. B **31**, 6832 (1985).
[2]W. Kirstein, B. Krüger, and F. Thieme, Surf. Sci. **176**, 505 (1986).
[3]J. Tersoff and L. M. Falicov, Phys. Rev. B **26**, 6186 (1982).
[4]X. Zhu, H. Huang, and J. Hermanson, Phys. Rev. B **29**, 3009 (1984); D. Wang, A. J. Freeman, and H. Krakauer, *ibid.* **24**, 1126 (1981).
[5]M. Weinert and J. Davenport, Phys. Rev. Lett. **54**, 1547 (1985).
[6]J. Tersoff and L. M. Falicov, Phys. Rev. B **24**, 754 (1981).
[7]K. Christmann, Surf. Sci. Rep. **9**, 1 (1988); J. W. Davenport and P. J. Estrup, in *Chemisorption Systems Part A. The Chemical Physics of Solid Surfaces and Heterogeneous Catalysis, Vol. 3A,* edited by D. A. King and D. P. Woodruff (North-Holland, Amsterdam, in press), and references therein.
[8]W. Eberhardt, F. Greuter, and E. W. Plummer, Phys. Rev. Lett. **46**, 1081 (1981); F. Greuter, I. Strathy, E. W. Plummer, and W. Eberhardt, Phys. Rev. B **33**, 736 (1986).
[9]F. Greuter and E. W. Plummer, Solid State Commun. **48**, 37 (1983).
[10]M. Balooch, M. J. Cardillo, D. R. Miller, and R. E. Stickney, Surf. Sci. **46**, 358 (1974).
[11]G. Comsa and R. David, Surf. Sci. **117**, 77 (1982).
[12]S. G. Louie, Phys. Rev. Lett. **42**, 476 (1979).
[13]T. H. Upton and W. A. Goodard, Phys. Rev. Lett. **42**, 472 (1979).
[14]P. Feibelman, D. R. Hamann, and F. J. Himpsel, Phys. Rev. **22**, 1734 (1980).
[15]P. Nordlander, S. Holloway, and J. K. Nørskov, Surf. Sci. **136**, 59 (1984).
[16]C. Umrigar and J. W. Wilkins, Phys. Rev. Lett. **54**, 1551 (1985).
[17]M. Y. Chou and J. Chelikowsky, Phys. Rev. Lett. **59**, 1737 (1987).
[18]C. F. Melius, J. W. Moskowitz, A. P. Moretola, M. B. Baillie, and M. A. Ratner, Surf. Sci. **59**, 279 (1976).
[19]P. E. M. Siegbahn, M. R. A. Blomberg, and C. W. Bauschlicher, J. Chem. Phys. **81**, 2103 (1984).
[20]J. Harris and S. Andersson, Phys. Rev. Lett. **55**, 1583 (1985).
[21]T. H. Upton, J. Am. Chem. Soc. **106**, 1561 (1984).
[22]U. Gradmann, Ann. Phys. (Leipzig) **17**, 91 (1966).
[23]J. W. Matthews and J. L. Cawford, Thin Solid Films **5**, 187 (1970).
[24]J. A. Knapp, F. J. Himpsel, and D. E. Eastman, Phys. Rev. B **19**, 4952 (1979).
[25]S. L. Hulbert, P. D. Johnson, N. G. Stoffel, W. A. Royer, and N. V. Smith, Phys. Rev. B **31**, 6815 (1985); W. Jacob, V. Dose, U. Kolac, Th. Fauster, and A. Goldmann, Z. Phys. B **63**, 459 (1986).
[26]S. Kevan, Phys. Rev. Lett. **50**, 526 (1983), and references therein.
[27]R. Dudde, U. Friess, K. H. Frank, and E. E. Koch, BESSY Annual Report, 1986 (unpublished).
[28]S. P. Tear and K. Röll, J. Phys. C **15**, 5521 (1982), and references therein.
[29]P. O. Gartland, S. Berge, and B. J. Slagsvold, Phys. Norveg. **7**, 39 (1983).
[30]B. Frick and K. Jacobi, Phys. Rev. B **37**, 4408 (1988).
[31]A. Goldmann, M. Donath, W. Altmann, and V. Dose, Phys. Rev. B **32**, 837 (1985).
[32]S. G. Louie, P. Thiry, R. Binchoux, Y. Petroff, D. Chandesris, and J. Lecante, Phys. Rev. Lett. **44**, 549 (1980); N. V. Smith, Appl. Surf. Sci. **22/23**, 349 (1985).
[33]F. J. Himpsel and D. E. Eastman, Phys. Rev. Lett. **41**, 507 (1978).
[34]G. D. Kubiak, Surf. Sci. **201**, L475 (1988).
[35]P. M. Echenique and J. B. Pendry, J. Phys. C **11**, 2065 (1978).
[36]A. Goldman, V. Dose, and G. Borstel, Phys. Rev. B **32**, 1971 (1985).
[37]N. V. Smith, Phys. Rev. B **32**, 3459 (1985).
[38]D. T. Pierce and H. C. Siegmann, Phys. Rev. B **9**, 4035 (1974).
[39]G. Bergmann, Phys. Rev. Lett. **41**, 264 (1978).
[40]R. Fournier and D. R. Salahub, Int. J. Quantum Chem. **29**, 1077 (1986).
[41]D. M. Newns, Phys. Rev. **178**, 1123 (1969).
[42]K. Schönhammer, Solid State Commun. **22**, 51 (1977).
[43]G. Doyen, D. Drakova, and F. von Trentini, in *Lectures on Surface Science,* edited by G. R. Castro and M. Cardona (Springer-Verlag, Berlin, York, 1978), p. 154.
[44]W. Reimer, Th. Fink and J. Küppers, Surf. Sci. **186**, 55 (1987).
[45]F. J. Himpsel, J. A. Knapp, and D. E. Eastman, Phys. Rev. B **19**, 2871 (1979).